Integration of Earth Observation and Geospatial Datasets for the Development of a National Multi-hazard Risk Assessment in Cyprus

Marios Tzouvaras [1,2]*, Constantinos Panagiotou [1], Nicholas Kyriakides [2], Maria Prodromou [1,2], Panagiotis Vasiliou [1], Marina Doukanari [1,2], Kyriaki Fotiou [1,2], Diofantos Hadjimitsis [1,2]

[1] ERATOSTHENES Centre of Excellence, Limassol 3012, Cyprus - marios.tzouvaras@eratosthenes.org.cy
[2] Department of Civil Engineering and Geomatics, Cyprus University of Technology, Limassol 3036, Cyprus - d.hadjimitsis@cut.ac.cy

Keywords: Disaster Risk Reduction, Geoinformatics, Earthquakes, Landslides, Fires, Floods.

Abstract

Cyprus is located in the Eastern Mediterranean region, which is an area exposed to multiple natural hazards including wildfires, floods, earthquakes and landslides. A comprehensive, approach for multi-hazard risk assessment is very essential for mitigation strategies in order to enhance resilience. This study integrates Earth Observation (EO) and geospatial datasets to assess and reduce multi-hazard risks, highlighting the role of remote sensing in vulnerability mapping. The proposed methodology combines Copernicus Sentinel-1 and Sentinel-2 satellite imagery and other auxiliary datasets, which are provided by national stakeholders, like the Department of Lands and Surveys, the Geological Survey Department, the Department of Forests, and the Water Development Department. Moreover, environmental variables derived from EO data, such as land use/land cover, vegetation indices, and topographic parameters, were analyzed to identify hazard vulnerable areas. The integration of these datasets provides a more accurate and holistic understanding of risks. The results derived from our approach show high accuracy compared to ground truth data, confirming the effectiveness of EO techniques in multi-hazard risk assessment. The study highlights the importance of geospatial technologies in disaster risk reduction and decision-making processes. By providing high-resolution, near-real-time data, EO-based approaches enable policymakers, stakeholders, and organizations to implement targeted mitigation measures.

1. Introduction

This study presents the integration of different EO techniques for assessing and reducing multi-hazards in Cyprus, which is located in the Eastern Mediterranean basin. This approach emphasizes the significance of EO and geospatial technologies in comprehensive vulnerability planning. The utilization of environmental factors derived from EO products provides valuable insight for policymakers, stakeholders, and organizations to enhance disaster assessment and improve risk reduction strategies.

Cyprus is located in the eastern part of the Mediterranean basin, exhibiting a unique geodynamic regime since its tectonic evolution is driven by interactions between the Eurasian and African plates. Besides its seismological interest, many active landslides and slope instabilities emerge because of the island's steep topography. Recently, climate change has led to the occurrence of more frequent and extreme flash floods. According to the European Commission, flooding is the most common and economical costly natural disaster at a European scale (EC, 2023), being responsible for destroying wetlands and urban areas, reducing biodiversity, degrading the soil health, etc. To address these issues, the EU authorities compiled the Flood Directive (2007/60/EC),) a legislation aiming to reduce the risks and the adverse effects of flooding on economy, environment, human health and cultural heritage (EC, 2007).

Wildfires are a serious threat to both the environment and human life. Their severity, frequency and capacity for destruction are determined by different factors, including climate change, human activities and the presence of flammable materials, also known as "fuel" (Tedim et al., 2018). Forest fires also occur frequently, especially during the dry period. Several factors contribute to the increased risk of wildfires including the prolonged and dry summers, strong winds, very steep slopes, vertical cliffs, deep gorges, narrow streams and long mountain ridges, highly flammable dry vegetation, increased urbanization coupled with the abandonment of rural areas (Turco et al., 2014). From 2001 to 2024, Cyprus lost significant tree cover due to fires, with 2021 being the worst year. Also, taking into account that the effect of the climate crisis unfolds, the frequency and intensity of climate-related disasters are increasing with a characteristic example, the year 2024, which has broken all existing records for the highest temperatures recorded on our warning planet, as a result, the presence of extreme wildfire events, storms, drought, etc. (FAO, 2023). Thus, focusing on wildfires, we are faced with the need for fire mitigation actions to avoid extreme fire events in the near future. The proposed methodology, which identifies the fire vulnerability areas, aims to significantly improve forest and fire management both nationally and internationally.

Remote Sensing is proven to be a valuable tool on disaster risk management since it provides spatiotemporal information over large areas (Shastry et al., 2023), supplementing the ground truth measurements. Thus, there is a great need for the development of multi-hazard risk assessment framework on a local, regional, and national level. This study is a first attempt to integrate Earth Observation (EO) and geospatial datasets for the development of a national multi-hazard risk assessment in Cyprus.

2. Data and Methodology

The multi-hazard risk assessment methodology deals with the monitoring and assessment of risks from the hazards with the

* Corresponding author

greatest impact in Cyprus, i.e., earthquakes, landslides, fires and floods. A variety of geospatial datasets and EO data exploiting the freely available Copernicus satellite data (Sentinel-1 and Sentinel-2) were used in the various layers developed. The data and methodology used for the production of the results of this study, are presented in this section.

2.1 Earthquakes

Seismic risk assessment for Cyprus is based on event-based probabilistic seismic risk analysis and eventual selection of seismic scenarios for given return periods. The current study was included in the 2018 National Risk Assessment of Cyprus (Cyprus Civil Defence, 2018), following the EC requirements and guidelines. This analysis is performed with the relevant algorithm of Openquake platform (Pagani et al., 2014; Silva et al., 2014), which first incorporates stochastic event-based hazard analysis for extended earthquake catalogues and models of the area.

The exposure model employed is built and elaborated by local resources, whereas the vulnerability model developed for local building typologies was used with additional considerations. The data used for the calculation of earthquake vulnerability are presented in Table 1 below.

Data	Source	Type	Resolution (m)
Geology	Cyprus Geological Survey Department (GSD)	Raster	50
Geological zones	GSD	Raster	50
Seismic zones	GSD	Raster	200
Seismological stations	GSD	Points	N/A
Construction material	Department of Town Planning and Housing	XLS, CSV	N/A
Number of floors		XLS, CSV	N/A
Year of construction		XLS, CSV	N/A

Table 1. Earthquake risk assessment parameters

2.2 Landslides

Landslide risk assessment was conducted using Multicriteria Decision Analysis (MCDA). The Analytic Hierarchy Process (AHP) (Saaty, 1980; Saaty, 1987) was used to assign weights to nine preselected factors influencing landslide susceptibility (Alexakis et al., 2014), namely slope, aspect, lithology, roads, relief, precipitation, land use, faults, and streams (Table 2).

A Digital Elevation Model (DEM) with 5m resolution was provided by the Department of Lands and Surveys of Cyprus (DLS), and used to derive geomorphological features, such as terrain slope, aspect, relief, and drainage network. In addition, lithology and faults data were provided by the Geological Survey Department of Cyprus (GSD). Additional open-access datasets, such as the European Space Agency (ESA) WorldCover 2021 (https://esa-worldcover.org/en) were utilized for classifying land use categories. Daily precipitation data for period 2011-2020 were collected from the Meteorological Department of Cyprus, whereas the spatial distribution of the road networks was provided by the DLS. The entire MCDA was performed using ArcGIS Pro, ensuring consistency and accuracy in the evaluation process. The final risk map was validated using a landslide inventory and hazard areas provided by the GSD.

Data	Source	Type	Resolution (m)
Land Cover	ESA Worldcover Version 2	Raster	10
Lithology	Cyprus Geological Survey Department (GSD)	Raster	50
Faults	GSD	Vector	N/A
Relief	Department of Lands and Surveys (DLS)	Raster	5
Slope	DLS	Raster	5
Aspect	DLS	Raster	5
Streams	DLS	Raster	5
Roads	DLS	Vector	N/A
Precipitation	Department of Meteorology	Raster	≈ 5,566

Table 2. Landslide risk assessment parameters

2.3 Fires

The fire risk assessment model was also developed using MCDA, whereas AHP was used to rank the criteria. Multiple types of data (Table 3) were processed from open-source databases to obtain information regarding the key fire factors, particularly from the Sentinel-2 mission to calculate NDVI and NDWI spectral indices, the Corine Land Monitoring Services to identify the land cover categories, the European Forest Fire Information System (EFFIS) to analyse fire history, and the Shuttle Radar Topography Mission (SRTM) data to extract topographical features. Information was also extracted from the National Opendata portal (https://data.gov.cy/) to delineate the picnic and camping sites, whereas the road network was obtained from the Global Roads Inventory Project (GRIP) website (http://www.globio.info/download-grip-dataset).

Data	Source	Type	Resolution (m)
NDVI	Sentinel 2	Raster	10
NDWI	Sentinel 2	Raster	10
Fire History	EFFIS	Vector	100
Slope	NASA SRTM Digital Elevation Model	Raster	30
Elevation		Raster	30
Aspect		Raster	30
Land Use/Land Cover (LULC)	Copernicus Corine 2018	Raster	100
Roads	Grip 4 Europe	Raster	1000
Temperature (LST)	Terra MODIS	Raster	1000
Camping sites	Department of Forests	Vector	50
Buildings	Microsoft	Vector	1

Table 3. Fire risk assessment parameters

For each parameter, the study area was divided into five distinct subregions based on their relevance to fire risk and combined with the criteria weights via the weighted linear combination (WLC) to calculate the fire risk index. The accuracy of the model was verified using fire data from the NASA-Fire Information for Resource Management System (FIRMS, https://firms.modaps.eosdis.nasa.gov/) and the European Forest Fire Information System (EFFIS, https://forest-fire.emergency.copernicus.eu/).

To ensure consistency and equal distribution across all parameters, values ranging from 0.1 to 1 were assigned. This approach ensures that all parameters are treated equally and makes them directly comparable. Factors identified as more significant were given a value of 1, while those considered less critical received a value of 0.1. This methodological approach, based on the Analytic Hierarchy Process (AHP), not only contributes to a fair evaluation process but also increases the accuracy of the weighting applied to each criterion.

2.4 Floods

Following the work of Kazakis et al. (2015), seven criteria (Table 4) and their associated weights were selected to assess flood susceptibility, particularly terrain elevation, terrain slope, flow accumulation, rainfall intensity, land-use land cover, soil (i.e., texture-depth) and distance from surface-water bodies (i.e., rivers, lakes, dams).

The MCDA framework proposed by Rahman et al. (2012) was adopted to identify regions that are highly prone to flood events in the non-occupied part of the Republic of Cyprus. In addition, the entire flood susceptibility analysis was conducted in R software. Prior performing the MCDA, the criteria maps are standardized between 0.1 and 1 to have a common scale based on literature survey and physical considerations, and projected into a common numerical grid with spatial resolution 500 m.

Data	Source	Type	Resolution (m)
Terrain elevation	Digital Elevation Model (DEM) from the Department of Land and Surveys (DLS)	Raster	25
Terrain slope		Raster	25
Flow accumulation		Raster	25
Rainfall Intensity	Department of Meteorology	XLS, CSV	N/A
Distance from drainage network	Water Development Department	Raster	N/A
Land Use/Land Cover	Corine Land Cover (CLC), 2018	Raster	100
Soil type	Geological Survey Department	Raster	1:25000

Table 4. Flood risk assessment parameters

The overall methodology, the data used, and the risk assessment results produced for the four hazards, i.e., earthquakes, landslides, fires and floods, are presented in the Figure 1 below.

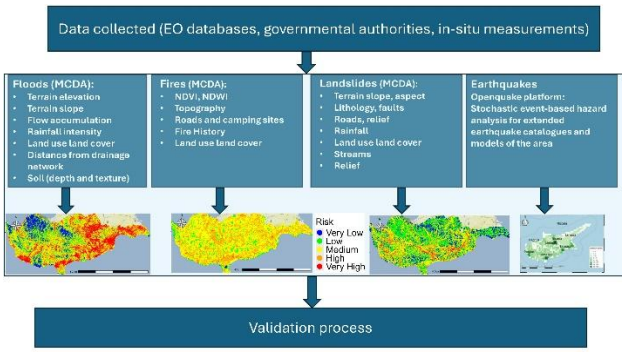

Figure 1. Risk assessment for earthquakes, landslides, fires and floods in Cyprus

3. Results and Discussion

3.1 Earthquakes

Earthquake risk is expressed in terms of monetary loss, at national level and the major cities. It is provided both in aggregated values and spatially distributed throughout Cyprus the island on maps. For the two scenarios, with 475 and 2500 years return period, expected casualties and displaced people are also calculated (Kazantzidou-Firtinidou et al., 2022).

The assessment of scenario damage and risk has been conducted for the specific earthquake scenarios, considering epistemic and aleatory uncertainties. Mean values and standard deviation were calculated for the buildings expected to be affected by the different damage states, for which the fragility curves have been determined (Kazantzidou-Firtinidou et al., 2019; 2022).

Figure 2a shows the number of buildings that are affected from various damage states for the two studied seismic scenarios. Approximately 83,000 buildings (25.64%) and 106,000 (32.52%) (% of the total building stock) for the T=475y and T=2500y scenario, respectively, are expected to reach the "Complete" damage state, whereas approximately 130,000 (40.07%) and 105,000 (32.19%) buildings are expected to present no damage at all (Kazantzidou-Firtinidou et al., 2022).

Furthermore, Figure 2b shows the ratio of collapsed buildings per structural typology, clearly presenting the most vulnerable ones. More than 30% of the stock of masonry and no ERD low-to-mid-rise typologies is expected to present damage at the level of collapse, in both scenarios. In the case of scenario T=2500y this ratio exceeds even 40%, a finding that is supported by the spatial distribution of PGA, affecting large zones and urban areas (Kazantzidou-Firtinidou et al., 2022).

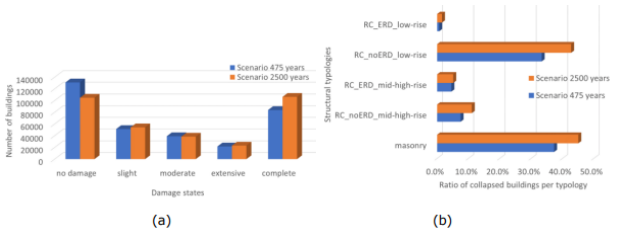

Figure 2. (a) Distribution of number of buildings per damage state and (b) ratio of collapsed 698 buildings ("complete") over total number of buildings per typology for the two scenarios. (Kazantzidou-Firtinidou et al., 2022)

Figure 3 shows the distribution of the aggregated economic loss per grid for the scenarios, i.e., T=475y (a) and T=2500y (b). Due the proximity of the fault for T=475y to Limassol and the high exposure value, Limassol and its outskirts are the most affected areas. For the scenario T=2500y, the affected areas are shifted to the west of Limassol, which aligns with the faults trace location (Kazantzidou-Firtinidou et al., 2022).

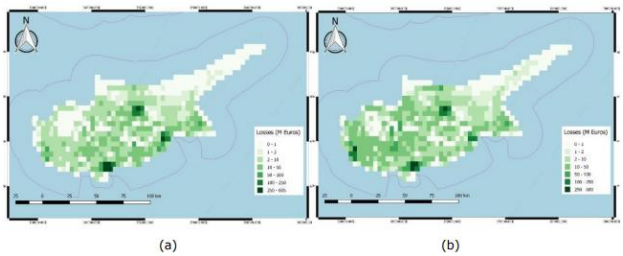

Figure 3. Loss map for seismic scenario with (a) T=475 years and (b) T=2500 years (Kazantzidou-Firtinidou et al., 2022)

While the total number of collapsed buildings may not show considerable variation, more significant levels of damage are detected in more structures and extended areas, which aligns with the distribution of loss. Among major urban centres, Limassol is expected to experience the greatest economic loss in both scenarios, due to the high concentrated damage and the high exposed replacement value. Each city's relevant area has been linked to the respective grid cells using the best possible spatial approximation. The monetary loss is significant throughout the island in both scenarios, as a considerable number of buildings are expected to be damaged and experience significant structural loss (Kazantzidou-Firtinidou et al., 2022).

The total amount is considerably greater than the results derived from the stochastic event-based approach for the corresponding return periods (T=475y, T=2500y), taking into account that the mean loss for the scenarios is calculated across the various simulations conducted within the event. In contrast, the event-based calculations utilise a single inter-event mean, and a sigma value associated with losses of a given return period (Kazantzidou-Firtinidou et al., 2022).

3.2 Landslides

The landslide risk map delineates areas of high and low susceptibility, providing a comprehensive visualization of potential hazards. High-risk zones, primarily characterized by steep slopes, unstable lithology, and proximity to fault lines, were identified as critical areas in need of immediate attention.

In contrast, low-risk regions displayed gentle terrain, stable geology, and minimal hydrological influence. This integrative approach significantly enhances the reliability of hazard assessments, aligning with established best practices in disaster risk management (Pourghasemi et al, 2012; Morales and de Vries, 2021).

The data were processed using the ArcGIS Pro, starting from the raw source data and undergoing a structured workflow to extract the necessary parameters. The spatial extent of each parameter was clipped to include only the areas of Cyprus under the effective control of the Republic of Cyprus. Subsequently, the parameters were classified according to their respective ranks and weights using the AHP method, as detailed in Table 5.

Parameter	Weight
Land Use/Land Cover	0.094
Lithology	0.013
Faults	0.079
Relief	0.245
Slope	0.026
Aspect	0.176
Streams	0.043
Roads	0.200
Precipitation	0.119

Table 5. Weights of landslide risk assessment parameters.

From the overall area, as indicated in Figure 4, 39% is categorised as low risk, while 14% is designated as extremely low risk. A significant portion, 31% of the total is classified as somewhat risky. Additionally, 13% of the region is identified as high risk, with the remaining 3% classified as very high risk, indicating critical zones prone to slope failures. These findings suggest that while a majority of the area has low to moderate susceptibility, high-risk zones require targeted mitigation strategies to reduce potential landslide hazards.

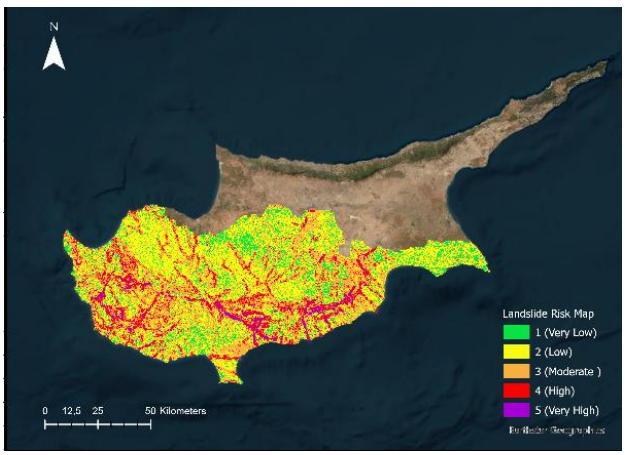

Figure 4. Landslide Vulnerability Index

The final landslide risk map was validated using a landslide inventory and hazard areas provided by the Geological Survey Department (GSD). The validation process assessed the spatial correlation between mapped high-risk zones and actual landslide occurrences. Results indicate that 74% of recorded landslides fall within high and very high-risk zones, demonstrating a good overall accuracy of the model.

This suggests that the risk map effectively identifies areas prone to landslides, making it a valuable tool for hazard assessment and mitigation planning. However, the remaining 26% of landslides occurring outside these zones highlights potential areas for refinement, such as improving input data resolution, adjusting classification thresholds, or incorporating additional influencing factors.

3.3 Fires

Based on the pairwise comparison using the AHP approach for the selected parameters, the derived weights are shown in Table 6. The consistency of the model was checked based on the CR which achieved 5.3%, which is below the commonly accepted threshold of 10% that means the pairwise comparison is consistent. As shown in Table 6, the highest weighted values are associated with Land Use/Land Cover, NDVI, and Fire History. This reinforces the significance of vegetation as a critical fuel source, confirming its role as a key factor in the initiation of fire events.

Parameter	Weight
NDVI	12.7
NDWI	6.1
Fire History	12.7
Slope	8.3
Elevation	6.4
Aspect	5.1
LULC	14.5
Roads	10.0
LST	6.5
Camping sites	8.2
Buildings	9.5
CI: 0.080, CR: 0.053	

Table 6. Weights assigned to the fire risk assessment factors.

The results of the fire risk assessment reveal significant variations in fire vulnerability across the study area, as shown in Figure 5. High and very high-risk zones are primarily found in shrublands, agricultural areas, grasslands, and forests, indicating their susceptibility due to vegetation and topographic complexity. In contrast, low-risk areas are mainly located in non-vegetated regions, such as water bodies and bare soils. These findings offer essential insights for decision-making.

During the selected period, the results indicate that 45% of the total area falls into the medium-risk class, 24% is classified as low risk, 22% as high risk, 7% as very low risk, and the remaining percentage as very high risk. This suggests that the area is vulnerable to the occurrence of fires.

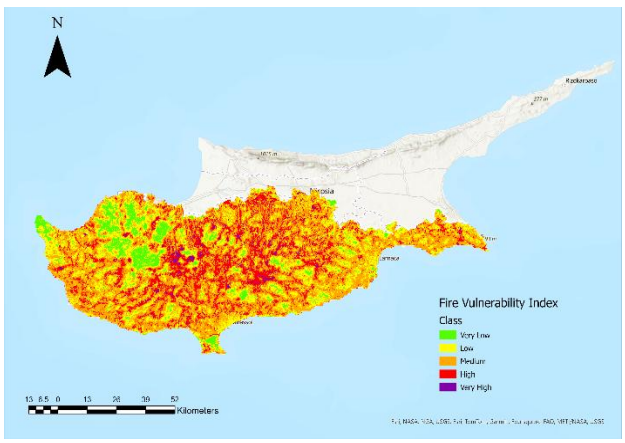

Figure 5. Fire Vulnerability Index

Additionally, the model was validated using historical fire events, which were compared against the calculated Vulnerability Index. This validation process ensures the model's reliability and effectiveness in assessing fire risk. By employing this approach, the model achieves a high Overall Accuracy of 87.14%, demonstrating its robustness in estimating the vulnerability and providing reliable risk assessments.

3.4 Floods

The standardized scores of the selected criteria are combined with the weight coefficients, shown in Table 7, via weighted linear combination to calculate the flood susceptibility levels at each location. The resulting susceptibility values are then classified into five distinct levels of risk based on their frequency distribution (histograms), with special attention on mitigating the impact of extreme values (outliers).

Parameter	Weight
Terrain elevation	0.21
Terrain slope	0.05
Land-use land cover	0.12
Distance from drainage network	0.21
Rainfall intensity	0.10
Soil	0.03
Flow accumulation	0.30

Table 7. Weights assigned to the flood risk assessment factors, adopted from Kazakis et al. (2015).

Figure 6 shows the spatial patterns of the flood susceptibility indicator, revealing that highly susceptible regions are present in the central-eastern part and the southern coastal part of the island because of the presence of urban areas, flattened terrains and medium soil permeability. On the other hand, the mountainous regions exhibit low susceptibility to flood events due to the high terrain slopes and the presence of dense forests. The resulting map is in very good agreement with the existing flood risk map, which is used by the water authorities (91%), supporting the validity of the proposed methodology.

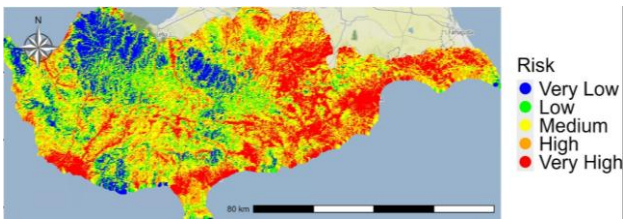

Figure 6. Flood Vulnerability Index

4. Conclusions

In this study, Copernicus Sentinel-1 and Sentinel-2 satellite data were used along with auxiliary data provided by various stakeholders/end-users in Cyprus, such as the Department of Lands and Surveys, the Department of Geological Survey Department, the Department of Forests and the Water Development Department. Moreover, environmental variables derived from Earth Observation data, such as land use/land cover, vegetation indices, and topographic parameters, were

calculated to identify hazard vulnerable areas. The integration of these datasets provided a more accurate and holistic understanding of risks.

For specific natural hazards under study, common parameters, i.e., elevation, aspect, relief, land use/land cover, precipitation, etc., were included in the analysis, however, the combination of parameters and their importance (weight) differs according to the natural hazard under investigation. This in fact highlighted the influence that each parameter has in the occurrence of such an event.

The resulting risk maps exhibit good agreement with existing studies and have been validated during bilateral discussions with relevant stakeholders. Indeed, the results derived from this study show high accuracy compared to ground truth data, ranging from 74% to 91%, confirming the effectiveness of EO techniques in multi-hazard risk assessment.

In the future, the use of Very High-Resolution satellite data from ESA Third Party Missions and the integration of Machine Learning techniques in the methodology will be investigated to further improve the accuracy. Last but not least, a combined multi-hazard risk index will be developed to assist stakeholders and end-users, from the public and private sector, in the decision-making process and the adoption and implementation of mitigation measures in an effort to reduce the impact of these disasters.

Acknowledgements

The present work is carried out in the framework of the ‘EXCELSIOR’: ERATOSTHENES: Excellence Research Centre for Earth Surveillance and Space-Based Monitoring of the Environment H2020 Widespread Teaming project (www.excelsior2020.eu) in which the Eratosthenes Centre of Excellence has been established. The ‘EXCELSIOR’ project has received funding from the European Union’s Horizon 2020 research and innovation programme under Grant Agreement No 857510, from the Government of the Republic of Cyprus through the Directorate General for the European Programmes, Coordination and Development and the Cyprus University of Technology. The authors also acknowledge the AI-OBSERVER project (https://ai-observer.eu/) that has received funding from the European Union’s Horizon Europe Framework Programme HORIZONWIDERA-2021-ACCESS-03 (Twinning) under the Grant Agreement No 101079468.

References

Alexakis, D.D., Agapiou, A., Tzouvaras, M., Themistocleous, K., Neocleous, K., Michaelides, S., Hadjimitsis, D.G., 2014. Integrated use of GIS and remote sensing for monitoring landslides in transportation pavements: the case study of Paphos area in Cyprus. Natural Hazards 72, 119–141. https://doi.org/10.1007/s11069-013-0770-3.

Civil Defence, 2018. National Risk Assessment for the Republic of Cyprus. Available at: https://www.moi.gov.cy/MOI/CD/cd.nsf/All/1D4A8C4AE68591AAC2258589003088E7?OpenDocument (29 November 2024).

European Commission, 2007. Directive 2007/60/EC of the European Parliament and of the Council of 23 October 2007 on the assessment and management of flood risks. Available at: https://eur-lex.europa.eu/eli/dir/2007/60/oj (27 November 2024).

European Commission, 2023. Floods. Available at: https://environment.ec.europa.eu/topics/water/floods_en#more-information (28 November 2024).

Food and Agriculture Organization, 2023. The Impact of Disasters on Agriculture and Food Security 2023, Avoiding and Reducing Losses through Investment in Resilience; FAO: Rome, Italy; ISBN 978-92-5-138194-6. https://doi.org/10.4060/cc7900en.

Kazakis, N., Kougias, I., Patsialis, T., 2015. Assessment of flood hazard areas at a regional scale using an index-based approach and Analytical Hierarchy Process: Application in Rhodope–Evros region, Greece, Science of The Total Environment, vol. 538, 555-563, https://doi.org/10.1016/j.scitotenv.2015.08.055.

Kazantzidou-Firtinidou D., Kyriakides N., Chrysostomou C., 2019. Earthquake Risk Assessment for Cyprus. 2nd international conference on natural hazard and infrastructure, 23–26 June, Chania. https://hdl.handle.net/20.500.14279/34263.

Kazantzidou-Firtinidou, D., Kyriakides, N., Votsis, R. et al., 2022. Seismic risk assessment as part of the National Risk Assessment for the Republic of Cyprus: from probabilistic to scenario-based approach. Nat Hazards 112, 665–695. https://doi.org/10.1007/s11069-021-05200-y.

Morales, F.F., de Vries, W.T., 2021. Establishment of Natural Hazards Mapping Criteria Using Analytic Hierarchy Process. Frontiers in Sustainability, 2, Article 667105. https://doi.org/10.3389/frsus.2021.667105.

Pagani, M., Monelli, D., Weatherill, G., Danciu, L., Crowley, H., Silva, V., Henshaw, P., Butler, L., Nastasi, M., Panzeri, L., Simionato, M., Vigano, D., 2014. “OpenQuake Engine: An open hazard (and risk) software for the Global Earthquake Model,” Seismological Research Letters, Vol. 85, No. 3, pp 692-702. https://doi.org/10.1785/0220130087.

Pourghasemi, H.R., Pradhan, B. & Gokceoglu, C., 2012. Application of fuzzy logic and analytical hierarchy process (AHP) to landslide susceptibility mapping at Haraz watershed, Iran. Natural Hazards 63, pp.965–996. https://doi.org/10.1007/s11069-012-0217-2

Rahman, M.A., Rusteberg, B., Gogu, R.C., Lobo Ferreira, J.P., Sauter, M., 2012. A new spatial multi-criteria decision support tool for site selection for implementation of managed aquifer recharge. Journal of Environmental Management, 99, 61-75. https://doi.org/10.1016/j.jenvman.2012.01.003.

Saaty, T.L., 1980. The analytic hierarchy process (AHP). The Journal of the Operational Research Society, 41(11), pp.1073-1076.

Saaty, R.W., 1987. The analytic hierarchy process–what it is and how it is used. Mathematical Modelling, 9(3-5), pp.161-176. https://doi.org/10.1016/0270-0255(87)90473-8.

Shastry, A., Carter, E., Coltin, B., Sleeter, R., McMichael, S., Eggleston, J., 2023. Mapping floods from remote sensing data and quantifying the effects of surface obstruction by clouds and

vegetation. Remote Sensing of Environment, 291, 113556, https://doi.org/10.1016/j.rse.2023.113556.

Silva, V., Crowley, H., Pagani, M., Monelli, D., Pinho, R., 2014. Development of the OpenQuake engine, the Global Earthquake Model's open-source software for seismic risk assessment. Natural Hazards 72, pp.1409-1427. https://doi.org/10.1007/s11069-013-0618-x.

Tedim, F., Leone, V., Amraoui, M., Bouillon, C., Coughlan, M.R., Delogu, G.M., Fernandes, P.M., Ferreira, C., McCaffrey, S., McGee, T.K., et al., 2018. Defining Extreme Wildfire Events: Difficulties, Challenges, and Impacts. Fire, 1(1), 9. https://doi.org/10.3390/fire1010009.

Turco, M., Llasat, MC., von Hardenberg, J., Provenzale, A., 2014. Climate change impacts on wildfires in a Mediterranean environment. Climatic Change 125, pp.369–380. https://doi.org/10.1007/s10584-014-1183-3.